Fuel 265 (2020) 117010

Contents lists available at ScienceDirect

Fuel

journal homepage: www.elsevier.com/locate/fuel

Full Length Article

Research on performance optimization and fuel-saving mechanism of an Atkinson cycle gasoline engine at low speed and part load

Niu Qingyu[a], Sun Baigang[a,*], Zhang Dongsheng[a,b], Luo Qinghe[a]

[a] School of Mechanical Engineering, Beijing Institute of Technology, Beijing 100081, China
[b] Beiqi Foton Motor Co., Ltd, Beijing 102206, China

ARTICLE INFO

Keywords:
HEV
Atkinson cycle
Compression ratio
LIVC
Optimization
Fuel economy

ABSTRACT

The Atkinson cycle engine plays a key role in the development of hybrid electronic vehicle (HEV) because of greater fuel economy than Otto cycle engine. The thermodynamic analysis shows Atkinson cycle has the significant advantage of cycle efficiency and the ratio of expansion ratio to effective compression ratio and pressure rise ratio have great influence on efficiency. A performance optimization strategy for the Atkinson cycle engine is proposed through analysis of compression ratio range according to cycle efficiency at small pressure rise ratio and optimization of the high compression ratio and the late intake valve closure (LIVC) under the compression pressure constraint. The experimental results show significant improvements in pumping losses and fuel economy are achieved, thus verifying verifies the effectiveness of the optimization strategy and brake specific fuel consumption (BSFC) of is improved by 9% at 2000 rpm@2 bar and 8% at 3000 rpm@3 bar, respectively. The fuel-saving mechanism is investigated in depth. The increase of mechanical efficiency due to the reduction in pumping mean effective pressure (PMEP) is the main reason for the fuel economy improvement at low and medium load, while the increase of indicated thermal efficiency is the main reason at high load. The increase in intake pressure is the main reason for the decrease in PMEP. The Atkinson cycle engine can achieve more obvious constant volume combustion and the combustion quality has been greatly improved. These findings can be used as guidelines for the development of new Atkinson cycle engines.

1. Introduction

Rising fuel price and the need of pollutant emission reduction and urban air quality improvement urgently require the development of efficient and low-emission green automobile products. HEVs can effectively reach the power, fuel economy and pollutant emission requirements during operating conditions, which is an effective technical solution for the automotive industry. In the urban driving cycle, most passenger cars operate at part load for more than 50% of the working time [1]. Because the traditional gasoline engine has some shortcomings such as large pumping loss and poor fuel economy at part load, it can no longer meet the demand of HEV for economy and emission. The Atkinson cycle engine has become the main choice for the development of HEV because of its own advantages [2]. Related research points out that 20%–30% of the fuel economy of HEV is attributed to the development and application of Atkinson cycle engine [3]. At present, it is generally believed that Atkinson cycle engine is an ideal engine type for hybrid power system [4].

Wang et al. [5] performed performance analysis and comparison of Atkinson cycle coupled with variable temperature heat sources based on maximum power and maximum power density conditions. Hou [6] compared the performance of air standard Atkinson and Otto cycle with heat transfer considerations including combustion constant, compression ratio and intake air temperature. He found that Atkinson cycle has greater work output and higher thermal efficiency than Otto cycle at the same operating condition. Gonca [7] conducted a theoretical study of the performance of the dual Atkinson cycle, considering heat transfer and friction losses. The effective power and power density rise to a specified value and then begin to decrease as the geometric compression ratio increases. Martins et al. [8] compared traditional gasoline engines, gasoline direct injection engines, diesel engines and Atkinson engines, and concluded that Atkinson cycle thermal efficiency reached nearly 75% at load of 30%–40%, which is 10% more than Otto cycle. Atkinson cycle was adopted to have the higher efficiency of range extender compared to conventional Otto cycle [9]. Zhao et al. [10] performed performance analysis and proposed the optimal parameters of the Atkinson cycle engine. Zhao et al. [11] indicated that the optimal value of the geometric compression ratio significantly optimizes the

* Corresponding author.
E-mail address: sunbg@bit.edu.cn (B. Sun).

https://doi.org/10.1016/j.fuel.2020.117010
Received 9 September 2019; Received in revised form 21 November 2019; Accepted 2 January 2020

classical Atkinson cycle performance. Little publication focused on the effect of the ratio of expansion ratio to effective compression ratio as a whole on Atkinson cycle efficiency. The effect of the ratio of expansion ratio to effective compression ratio on Atkinson cycle efficiency is investigated by thermodynamic analysis and the range of geometric compression ratio is proposed for the Atkinson cycle engine.

Wei et al. [12] investigated the combustion process and emission characteristics of Miller cycle diesel engine at medium and low loads by three-dimensional simulation. Zhao et al. [13] proposed a part load fuel economy optimization method for Atkinson cycle engine based on one-dimensional engine simulation model. By conducting Matlab-Simulink and GT-Suite coupling simulations, the proposed variable Atkinson cycle contributed to efficiency improvements of the engine at partial loads [14]. The LIVC of Atkinson cycle will reduce engine power and need to be compensated by increasing the compression ratio of Atkinson cycle engine, but increasing the compression ratio may lead to engine knock. Li et al. [15] found that Atkinson cycle would alleviate engine knock problem with lowered temperature and pressure of the air–fuel mixture before combustion. Molina et al. [16] indicated that the Miller strategy is able to extend the ignition delay and reduce pressure gradients because of the lowering of in-cylinder temperatures. Wei et al. [17] found that LIVC and EIVC can efficiently suppress knock. Little publication focused on performance optimization about the high compression ratio and LIVC of Atkinson cycle engine. Based on the compression ratio range of Atkinson cycle from thermodynamic analysis, the performance optimization strategy of Atkinson cycle engine is proposed, that is to get the design principle relationship between CR and intake valve timing under the constraint of compression pressure, and to optimize CR and other valve timing.

Mallikarjuna et al. [18] made theoretical and experimental research on Atkinson engine with an effective compression ratio of 8:1, the research results have shown that at part load conditions, the pumping loss can be reduced by 43%. Cao [19], Zaccardi et al. [20], Gheorghiu [21], Watanabe et al. [22], and Westbrook et al. [23] theoretically and experimentally studied Atkinson gasoline engine and found it a significant improvement thermal efficiency compared with that of conventional engines. Matsuo et al. [24] showed that the fourth-generation Prius Atkinson engine is the world's first gasoline engine to achieve 40% thermal efficiency. Ohn et al. [25] found that Atkinson gasoline engine has an indicative fuel consumption rate that is 10% lower than conventional gasoline engines of the same specification. Pertl et al. [26] analyzed combustion, emission and fuel consumption of the Atkinson cycle engine and concluded that a small internal combustion engine using the Atkinson cycle may be an alternative to future internal combustion engine applications. Zhao et al. [27] found that after re-optimizing the variable valve timing (VVT) and applying the LIVC, the pumping losses significantly decrease and the fuel economy is obviously improved. However, for a high compression ratio Atkinson cycle engine, the effect of increasing the indicated thermal efficiency on fuel economy at medium and high load cannot be ignored. Little publication focused on the effect of the indicated thermal efficiency for Atkinson cycle engine and its relationship with the mechanical efficiency on the fuel economy of Atkinson cycle engine. Therefore, the fuel-saving mechanism of Atkinson cycle engine is investigated in great detail at low speed and part load compared with the experimental data of the original engine.

The purpose of this paper is to introduce a novel performance optimization strategy for the Atkinson cycle engines and investigate the fuel-saving mechanism of the Atkinson cycle engines in great detail at low speed and part load. The test equipment and process is presented in session 2.1 and the one-dimensional simulation engine model is established and validated in session 2.2. In session 3.1, the effect of the ratio of expansion ratio to effective compression ratio on Atkinson cycle efficiency is investigated by thermodynamic analysis and the range of geometric compression ratio is proposed for Atkinson cycle engine; through one-dimensional simulation, the optimization strategy of the high compression ratio and LIVC under the compression pressure constraint is presented and the CR and other valve timing is optimized in session 3.2; the experimental results verifies the effectiveness of the optimization strategy and the fuel-saving mechanism of Atkinson cycle engine is investigated in depth in session 3.3. These findings can be used as guidelines in Atkinson cycle engines and indicate the direction for the development of new Atkinson cycle engines.

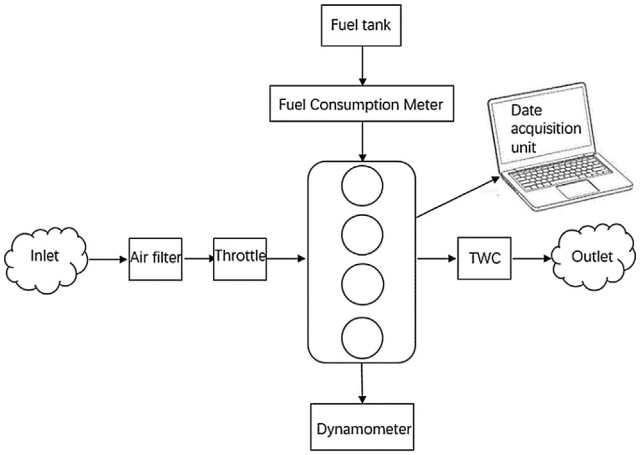

Fig. 1. Schematic view of the engine bench.

2. Materials and method

2.1. Test equipment and process

The engine test bench is shown in Fig. 1. The test cell included DYNAS3 LI 250 high dynamic electric dynamometer. The engine speed, engine oil temperature, coolant temperature, and intake air temperature were recorded automatically from the dynamometer control console. The cylinder pressure was measured using a Kislter 6117B pressure sensor with an accuracy of ± 1.25 bar, and the crank angle position was specified by Kislter 2613B crank angle encoder which can measure 0–20,000 rpm and the accuracy can reach to 0.1 °CA. The cylinder pressure and the corresponding crank angle were captured through AVL621 combustion analyzer. FC2210Z intelligent fuel consumption meter with an accuracy of ± 0.5% and Horiba air fuel ratio tester with a measurement accuracy of ± 0.1% was used in the test. Tests were conducted after running the engine until it reached a steady state at an oil temperature of 90 °C and cooling water temperature of 80 °C. During the test, the coolant outlet temperature was controlled at 88 ± 5 °C, the oil temperature was controlled below 135 °C, and the total exhaust temperature was controlled below 850 °C.

The original Otto cycle engine was tested in the bench and the main specifications are shown in Table 1. Then, in order to achieve Atkinson cycle, the camshaft is replaced by a long intake camshaft, and the original piston is replaced by a new piston with high geometric compression ratio. Based on the above improvements, the Atkinson cycle engine is adjusted in real time by VVT according to engine speed and load.

2.2. Simulation model and validation

The performance optimization of the Atkinson cycle engine is based on a simulation model of a1.6L gasoline engine using the one-dimensional simulation Ricardo WAVE software. The simulation model includes four sub-models: geometry, combustion, heat transfer, and friction models. According to the main technical parameters, the gasoline engine is simplified into modules consisting of the intake system, the exhaust system, the combustion system, the fuel injection system, the environmental boundary and the corresponding connecting pipelines.

Table 1
Engine specifications.

Parameter	Value
Type	Inline, water cooled
Number of Cylinders	4
Bore	78 mm
Stroke	83.6 mm
Connecting rod length	134.7 mm
Displacement	1.6 L
Compression ratio	10.4
Diameter of the intake valve/Max lift	32/9 mm
Diameter of the exhaust valve/Max lift	26.8/9 mm
Number of Intake Valves/Exhaust valves	2/2
Allowable Maximum combustion pressure	80 bar
Max Torque/Speed	150 N.m/5000 rpm
Rated Power/Speed	81 kW/5500 rpm

The corresponding physical model is established. The SI Wiebe, Woschni heat transfer and Chen-Flynn Friction models were employed for the combustion, heat transfer and friction processes, respectively.

2.2.1. Details of the combustion model

The Wiebe function is often used to approximate the actual heat release characteristic of the engine [28]. The cumulative mass fraction burned as a function of crank angle is given by the following:

$$W = 1.0 - exp(-AWI\,(\theta/BDUR)^{WEXP+1}) \tag{1}$$

where *AWI* is internally calculated parameter to allow *BDUR* to cover the range of 10–90%; θ is degrees past start of combustion; *BDUR* is user-entered combustion duration (10–90%); *WEXP* is user-entered exponent in Wiebe function.

2.2.2. Details of the engine friction model

For calculation of engine friction, the Chen-Flynn Fiction model is used. The equation used to calculate friction is given below:

$$FMEP = A_{cf} + \sum_{i=1}^{ncyl} [B_{cf}(P_{max}) + C_{cf} * (S_{fact})_i + Q_{cf} * (S_{fact})_i^2] \tag{2}$$

$$S_{fact} = RPM * stoke/2 \tag{3}$$

where A_{cf}, B_{cf}, C_{cf}, Q_{cf} need user input according to parameters of the calculation engine (the value of *FMEP* is modified using the test data for this study); P_{max} is maximum cylinder pressure; *RPM* is cycle average engine speed; stroke is cylinder stroke.

2.2.3. Details of the heat transfer model

The heat transfer model used for the calculation is Woschni model which is available in the Boost software and this model calculates the heat transfer rates to the piston, cylinder head, and liner [29]. Wall temperatures are provided as the input to the heat transfer model.

2.2.4. Boundary conditions

The system boundary mainly sets the temperature, the pressure and other parameters. Temperature and pressure are the ambient temperature and pressure when the engine is working. The surface temperature of piston top is estimated to be 550 K, the surface temperature of cylinder head bottom is estimated to be 495 K, and the surface temperature of cylinder liner is estimated to be 450 K. The parameters for combustion model can be set according to the test data. The setting conditions and parameters of the model is shown in Table 2.

2.2.5. Model validation

The established engine calculation model is shown in Fig. 2. In order to verify the accuracy of the established calculation model, the model was simulated from 1500 rpm to 5500 rpm every 500 rpm to obtain the full load characteristic curve, which was compared with the test data curve.

Table 2
Boundary conditions.

Parameter	Value
Temperature of ambient (K)	293
Pressure of ambient (Bar)	1.01325
Temperature of piston top (K)	550
Temperature of cylinder head (K)	495
Temperature of cylinder liner (K)	450

In Fig. 3, it can be seen that the whole model is ideal in the full speed range. The simulation data is basically consistent with the test data. The error is less than 5% at each speed. It can be considered that the model is reasonable and can be used for subsequent calculation.

3. Results and discussion

3.1. Thermodynamic analysis of Atkinson cycle

Compared with Otto cycle, the expansion ratio of Atkinson cycle is greater than the effective compression ratio, and the expansion stroke can make more efficient use of the heat generated by the combustion. As shown in Fig. 4 1-2-3-4-5-1 describes the thermodynamic model of the Atkinson cycle, and 5′-2-3-4-5′ represents the thermodynamic model of the Otto cycle [30,31].

Atkinson cycle efficiency can be calculated as follows:

$$\eta = 1 - \frac{1}{\varepsilon_c^{k-1}} * \frac{(k-1)\frac{\varepsilon_e}{\varepsilon_c} + \delta\left(\frac{\varepsilon_e}{\varepsilon_c}\right)^{1-k} - k}{\delta - 1} \tag{4}$$

In Eq. (4), the Atkinson cycle effective compression ratio $\varepsilon_c = v_1/v_2$, the Atkinson cyclic expansion ratio $\varepsilon_e = v_4/v_3$, the pressure increase ratio $\delta = p_3/p_2$, and the adiabatic index $k = C_p/C_v$. It can be seen that Atkinson cycle efficiency depends not only on the effective compression ratio but also on expansion ratio and the pressure rise ratio. When $\varepsilon_e/\varepsilon_c = 1$, Otto cycle efficiency can be calculated as follows:

$$\eta = 1 - \frac{1}{\varepsilon_c^{k-1}} \tag{5}$$

To clearly illustrate the efficiency advantage of Atkinson cycle and study the influence factor of Atkinson cycle efficiency, computations were made to compare the results.

The engine pressure rise ratio varies with load, typically 1.5–3.5. Fig. 5 shows changes of Atkinson cycle efficiency with $\varepsilon_e/\varepsilon_c$ at different pressure rise ratios when ε_c is 10.4. The Atkinson cycle efficiency is greater than Otto cycle efficiency in the reasonable range of $\varepsilon_e/\varepsilon_c$. At different pressure rise ratios, the Atkinson efficiency increases first and then decreases with the increase of $\varepsilon_e/\varepsilon_c$. With the increase of pressure rise ratio, the maximum efficiency increases and the corresponding $\varepsilon_e/\varepsilon_c$ becomes larger. The decrease rate of Atkinson efficiency after the maximum value gradually decreases as pressure rise ratio increases. As shown in Fig. 5(b), it is closer to the real engine cycle when $k = 1.35$. It can be seen that the variation law is basically the same as that when $k = 1.4$. The value of the maximum efficiency is changed, while the position of the maximum efficiency remains unchanged at each pressure rise ratio.

As for the urban road driving, the vehicle engine is mainly operated at part load, so it is very important to improve thermal efficiency for part load. Therefore, the small pressure increase ratio is referenced as $\delta = 1.5$ for Atkinson cycle efficiency. The Atkinson maximum cyclic efficiency point $\varepsilon_e/\varepsilon_c = 1.35$ is obtained and the $\varepsilon_e/\varepsilon_c$ range of 1.15–1.35 is considered for the Atkinson cycle engine. The effective compression ratio of the Atkinson cycle engine is kept in accordance with the original compression ratio of 10.4. Further calculation shows that the expansion ratio range of Atkinson cycle is 12–14, so the compression ratio of the Atkinson cycle engine should be between 12 and

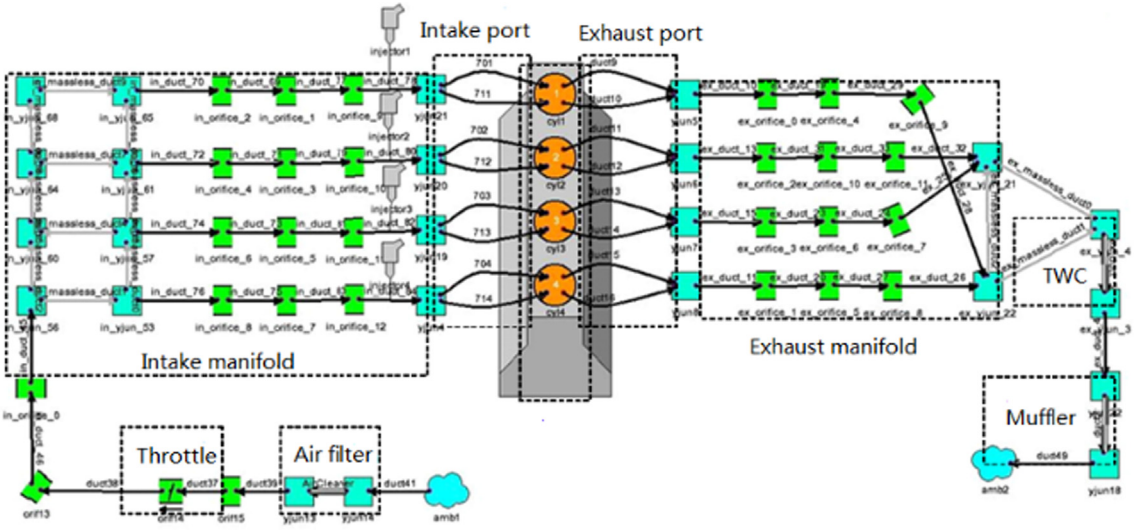

Fig. 2. Engine performance simulation model.

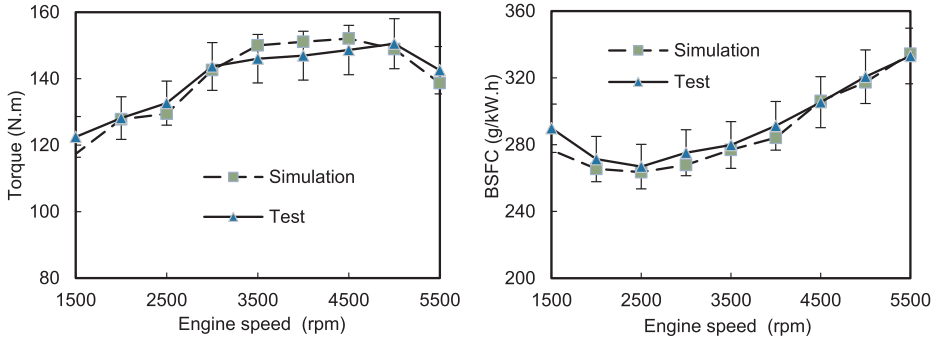

(a) Torque (b) BSFC

Fig. 3. Comparison of the torque and BSFC.

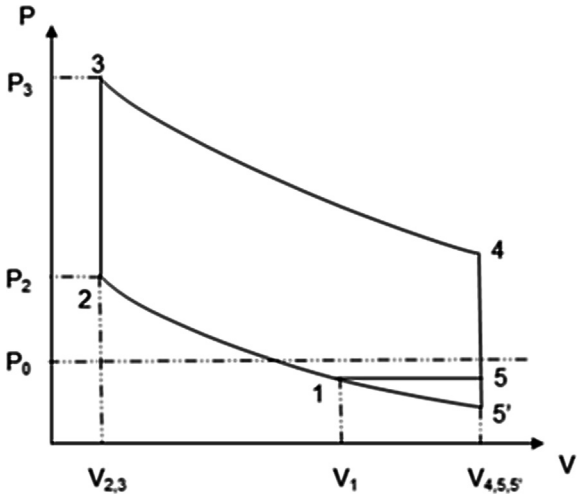

Fig. 4. Atkinson cycle and Otto cycle *p-v*.

14.

After defining the range of compression ratio of the Atkinson cycle engine, the intake valve timing also need to be changed. Excessive late intake valve closure angle will cause the power loss, and excessive early intake valve closure angle will cause the maximum explosive pressure of the engine to be too high or even cause the engine detonation when it is serious. So it is necessary to choose an appropriate intake valve closure to match the compression ratio.

3.2. Simulation optimization of the Atkinson cycle engine

3.2.1. Determination of the compression pressure

The cylinder pressure at compression top dead center is the main factor affecting the maximum explosive pressure and power of the engine. According to the engine performance simulation model, the duration of combustion is set to 14 °CA and 50% heat release point is set at 18 °CA ATDC, which makes the engine ignite and heat release after the compression top dead center, and obtains the pressure at top dead center of the original gasoline engine. It is calculated that the compression pressure at top dead center of the original gasoline engine is not more than 25–26 bar at each speed,

As shown in Fig. 6, when the compression ratio is increased to 13.5 directly, the compression pressure exceeds the range, resulting in an increase in detonation and mechanical loss. Therefore, while increasing the compression ratio, it is necessary to increase the closure angle of the intake valve so that a part of the working fluid can flow back to the intake manifold to ensure a reasonable compression pressure range.

3.2.2. Optimization of the IVC at compression ratios

The engine used on urban road is usually operated at low and medium speed conditions. The representative reference speed is 2500 rpm. Fig. 7 shows the relationship between the compression pressure and the intake valve closure angle at different compression ratios at 2500 rpm. 25 bar is used as the constraint condition of compression pressure.

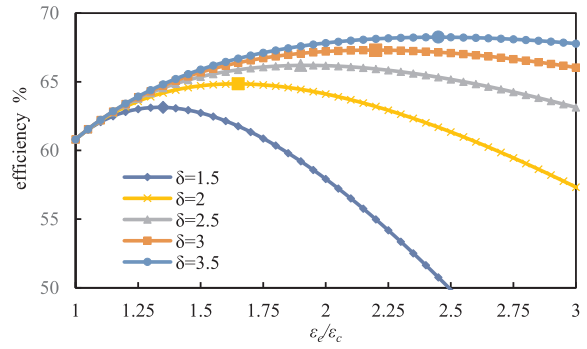

(a) k=1.4

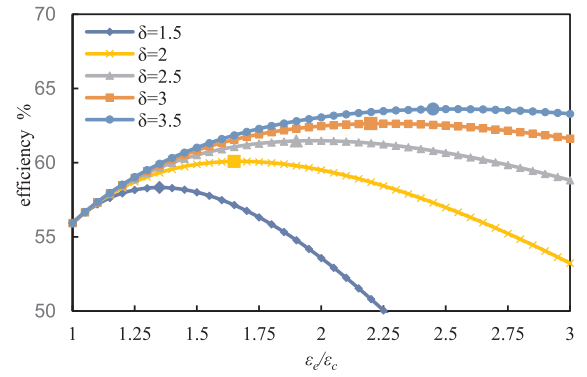

(b) k=1.35

Fig. 5. Changes of Atkinson efficiency with $\varepsilon_e/\varepsilon_c$ at different pressure rise ratios.

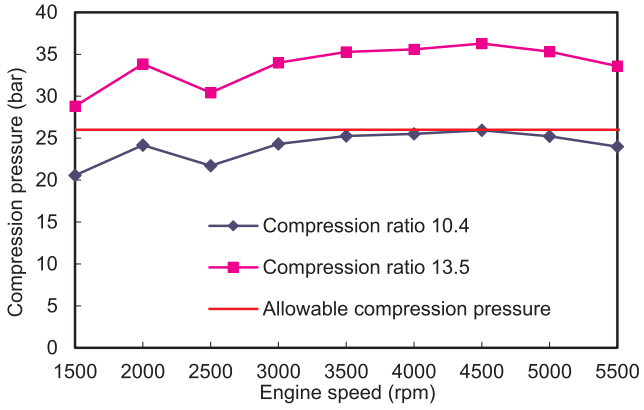

Fig. 6. Comparison of engine compression pressure.

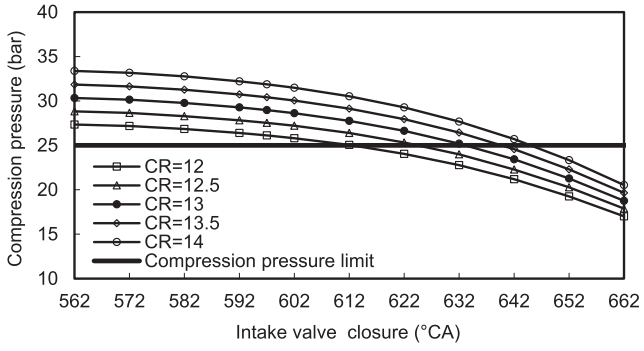

Fig. 7. Changes of compression pressure with IVC at 2500 rpm.

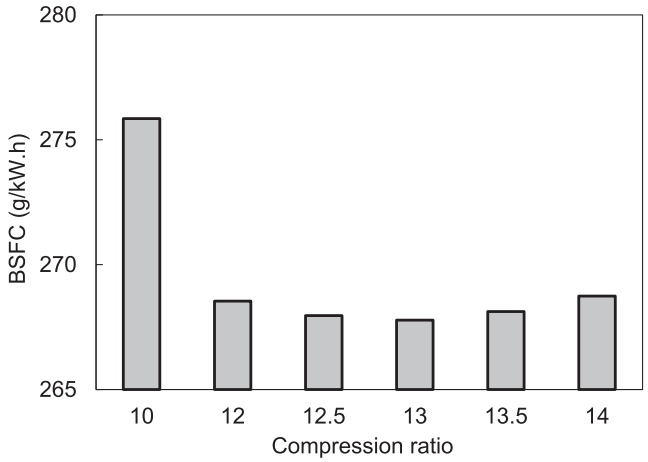

Fig. 8. Changes of BSFC with compression ratios at 2500 rpm.

As can be seen from Fig. 7, the compression pressure of the cylinder decreases as the intake valve closure angle is delayed when the compression ratio is constant, and the rate of decrease gradually increases. This is because as the intake valve closure angle is delayed, the amount of backflow of the in-cylinder mixture to the intake port increased, so that the amount of trapping mixture in the cylinder is reduced, thereby the pressure at the compression top dead center is reduced. And with the gradual delay of the closure angle of the intake valve, the amount of the mixture returning to the intake port increases faster and faster, and the amount of trapping mixture in the cylinder decreases more and more rapidly, so that the compression pressure is reduced faster and faster.

3.2.3. Optimization of the compression ratio and the other valve timing

According to the corresponding relationship, with the minimum fuel consumption as the optimum condition, the BSFC of the engine is simulated to determine the optimum relationship of compression ratio and IVC. As shown in Fig. 8, the BSFC decreases due to the increasing efficiency as the compression ratio increases from 10 to 13, while the BSFC increases as the compression ratio increases from 13 to 14. This is because the higher the compression ratio, the later the intake valve closure at a fixed compression pressure, which results in increased backflow and power loss. This reduces mechanical efficiency and increases fuel consumption at high compression ratio. Taking into account these factors, 13 is recommended as the compression ratio of Atkinson cycle engine.

After defining the constraint relationship between the intake valve closure angle and compression ratio, the other valve timings are optimized by simulation as below: the minimum pumping loss should be taken into account in the intake valve opening angle, and the maximum thermal efficiency should be taken into account in the exhaust valve opening angle. The closure angle of exhaust valve needs to consider both thermal efficiency and volumetric efficiency. For an actual engine, the optimal valve timing varies with operating conditions. In this work, the valve timing of Atkinson cycle engine can be optimized as the design point due to the VVT.

3.3. Analysis of experimental results and fuel-saving mechanism

3.3.1. Analysis on fuel economy at low speed

Fig. 9 shows comparison of BSFC of the Atkinson cycle engine and Otto cycle engine at 2000 rpm and 3000 rpm. BSFC of Atkinson cycle engine is less than that of Otto cycle engine at each load. The thermal efficiency is greatly improved which verifies effectiveness of the present strategy. The fuel saving rate of Atkinson cycle engine is getting smaller with the increase of load. The following is an in-depth analysis of the fuel saving reasons of Atkinson cycle engine.

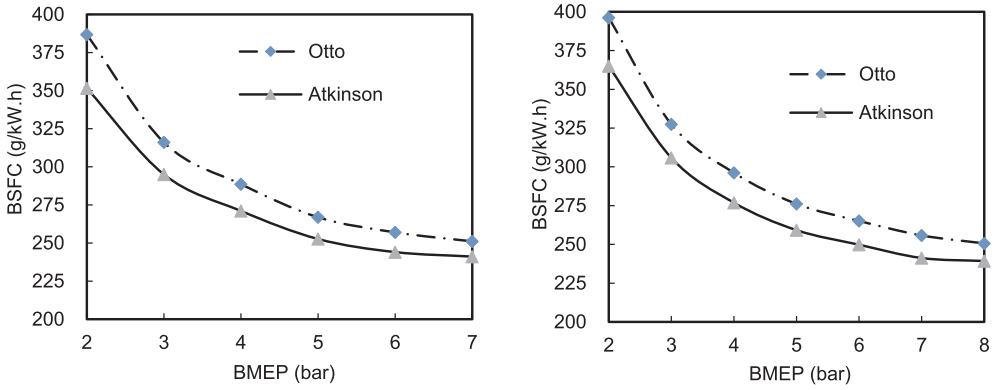

Fig. 9. Comparison of BSFC.

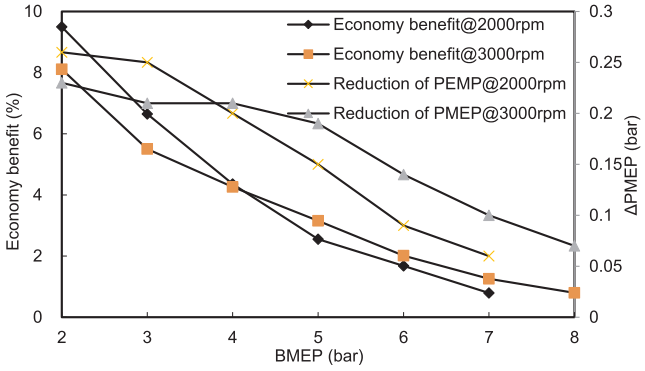

Fig. 10. Change of economy benefit and ΔPMEP with BMEP.

In order to evaluate fuel economy, the economy benefit from reduction of PMEP is defined as ΔPMEP/IMEP × 100%. Fig. 10 shows the change of economy benefit and ΔPMEP with BMEP. It can be seen that ΔPMEP and the economy benefit is getting smaller with the increase of load.

Fig. 11 presents the comparison of indicate thermal efficiency between Otto cycle engine and Atkinson cycle engine at different load. Improvement of indicate thermal efficiency can be about 2% at high load. The indicated thermal efficiency is the ratio of the indicated work of the actual cycle of the engine to the heat of the fuel consumed, i.e.$\eta_i = \frac{W_i}{Q}$, where Q is the heat of the fuel consumed to obtain the indicated work W_i. When the indicated power P_i and fuel consumption per hour B are measured for the engine, $\eta_i = \frac{3600P_i}{BH_u}$ can be obtained, where H_u is the low calorific value of fuel used. It can be seen from the above formula that under the specified fuel, it is only related to the indicated power Pi and fuel consumption B, wherein the loss of gas exchange process is not considered. In this study, P_i and B can be measured in the experiment and the indicated thermal efficiency we use in this paper is calculated by this method.

In order to discuss fuel economy mechanism of the Atkinson engine, Figs. 10 and 11 will be analyzed together. At low load, the throttle opening is small and the pumping loss of Otto cycle engine is very large. Atkinson cycle engine can significantly reduce the PMEP by delaying the intake valve closure and the economy benefit from reduction of PMEP is considerable. The indicated efficiency of Atkinson cycle engine is higher than of the Otto cycle engine, but the increase in indicated thermal efficiency is very limited. Therefore, the economy benefit at low load is caused by the reduction of PMEP and the improvement of indicated thermal efficiency. The increase of mechanical efficiency due to the reduction in PMEP is the main reason for the fuel economy improvement at low load.

As load increases to medium load, the throttle opening increases and the pumping loss of Otto cycle engine decreases, so the economy benefit from reduction of PMEP is lower than that at low load. The indicated efficiency of Atkinson engine is improved more than that at low load. Therefore, the economy benefit at medium load is caused by the reduction of PMEP and the improvement of indicated thermal efficiency. Because the relative increase of thermal efficiency is less than the relative decrease of economy benefit from PMEP reduction. The economy benefit of Atkinson cycle engine is lower compared with that at small load. The effect of the increase of indicated thermal efficiency

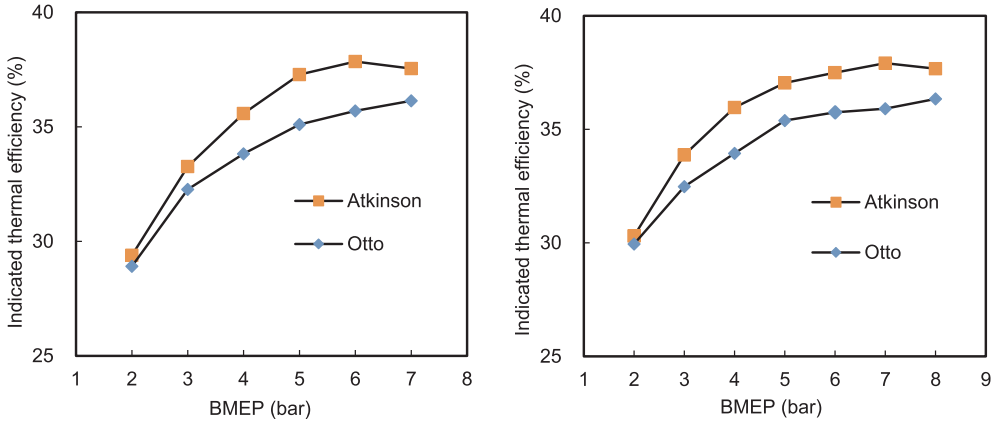

Fig. 11. Comparison of indicated thermal efficiency with BMEP.

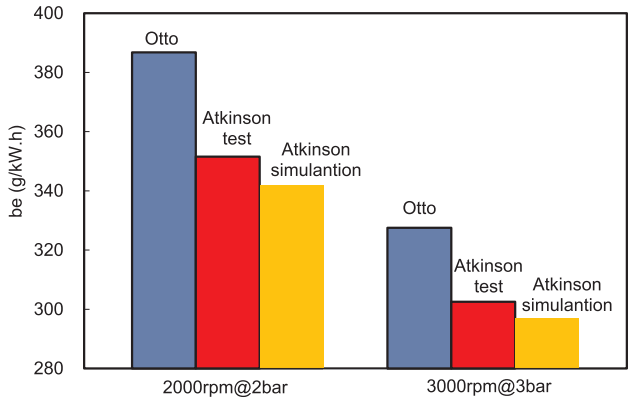

(a) BSFC

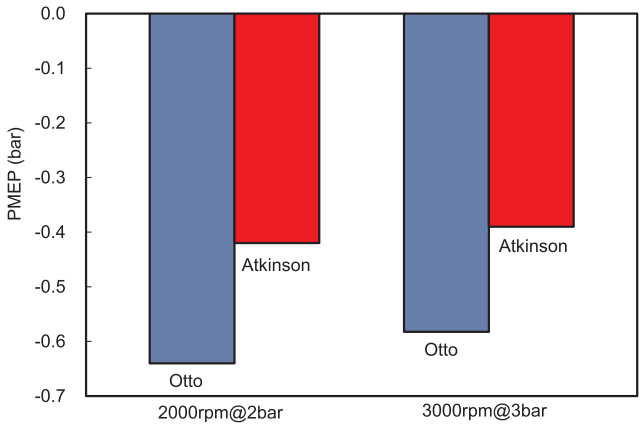

(b) PMEP

Fig. 12. Comparison of BSFC and PMEP.

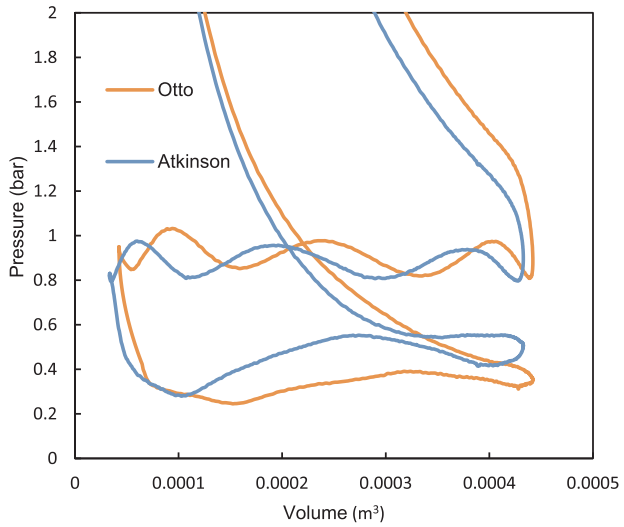

(a) 2000rpm@2bar

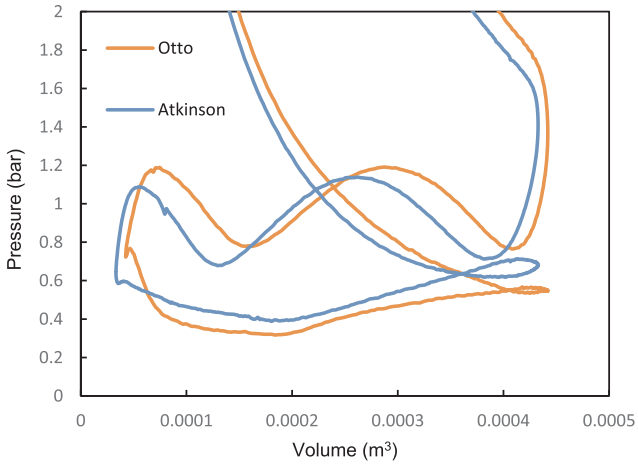

(b) 3000rpm@3bar

Fig. 13. Comparison of pumping-loop cylinder pressure.

is smaller than that of the increase of mechanical efficiency, so the increase of mechanical efficiency due to the reduction in PMEP is the main reason for the fuel economy improvement at medium load.

When the load is further increased to high load, the throttle opening is gradually approaching full and the pumping loss of the Otto cycle engine is very small. Compared with that at low and medium load, the economy benefit from reduction of PMEP continues to decrease and the indicated efficiency is improved more. Therefore, the economy benefit at high load is caused by the reduction of PMEP and the improvement of indicated thermal efficiency. Because the relative increase of thermal efficiency is less than the relative decrease of economy benefit from PMEP reduction. The economy benefit of Atkinson cycle engine is lower compared with that at medium load. The effect of the increase of indicated thermal efficiency is bigger than that of the increase of mechanical efficiency, so the increase of indicated thermal efficiency is the main reason for the fuel economy improvement at high load.

3.3.2. Analysis on fuel economy at typical working load

Fig. 12 shows the comparison of BSFC and PMEP of the original and Atkinson engine. At 2000 rpm@2 bar, the effective fuel consumption rate of the Atkinson cycle engine is 9% lower than that of the Otto cycle engine, and at 3000 rpm@3 bar, BSFC of the Atkinson cycle engine is 8% lower than that of Otto cycle engine. The comparison results between calculation and test at 2000 rpm@2 bar and 3000 rpm@3 bar are also shown in Fig. 12(a). It can be seen that the calculated BSFC of the Atkinson cycle engine are basically consistent with the test and the error is 2.7% and 1.8% respectively.

Pumping loss is the main reason for high fuel consumption rate of Otto cycle engine at low load. It can be seen that the PMEP and BSFC of Atkinson cycle engine are significantly reduced compared with that of Otto cycle engine.

In order to further understand the change of PMEP, the comparisons of pumping-loop cylinder pressure and intake manifold pressure are presented in Figs. 13 and 14. The cylinder pressure in the intake stroke of the Atkinson cycle engine is obviously higher at 2000 rpm@2 bar and 3000 rpm@3 bar as shown in Fig. 13. The intake pumping loss of the Atkinson cycle engine is reduced a lot. The difference of the cylinder pressure at 3000 rpm@3 bar is not obvious than that at 2000 rpm@2 bar. Therefore, although the PMEP is reduced, the extent is smaller. As a result, the fuel economy improves by 9% and 8%, respectively.

The comparison of intake pressure is presented in Fig. 14. The pressure in the intake manifolds increases contributing to the higher cylinder pressure in the intake stroke. The intake pressure of Atkinson cycle engine is generally higher than that of Otto cycle engine due to the late intake valve closure and the return flow of gas in cylinder, which eventually leads to a reduction in PMEP. Compared with 2000 rpm@2 bar, the intake pressure of the Atkinson cycle engine at 3000 rpm@3 bar, is still higher than that of Otto cycle engine, but the gap has narrowed.

The comparison of *P–V* diagram is presented in Fig. 15. The P_{max} of the Atkinson cycle engine is higher than that of the original engine and

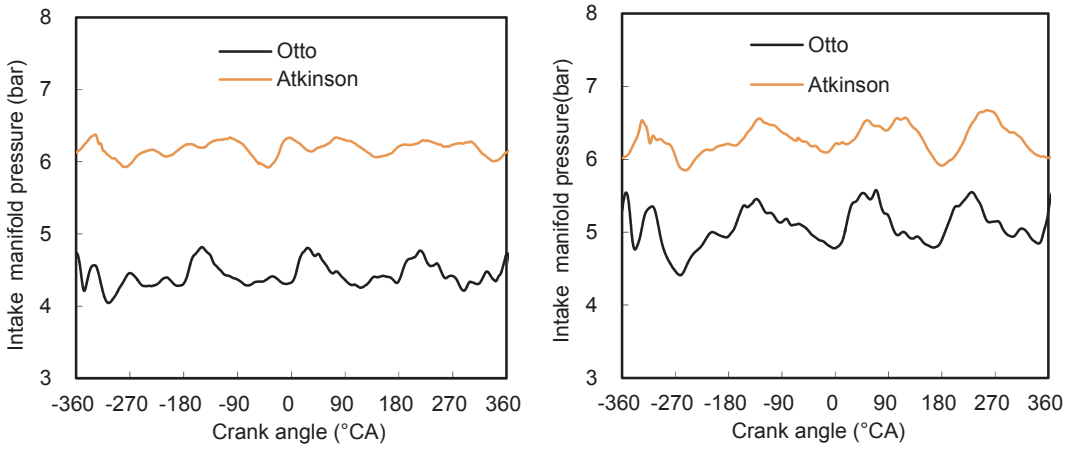

(a) 2000rpm@2bar (b) 3000rpm@3bar

Fig. 14. Comparison of intake pressure.

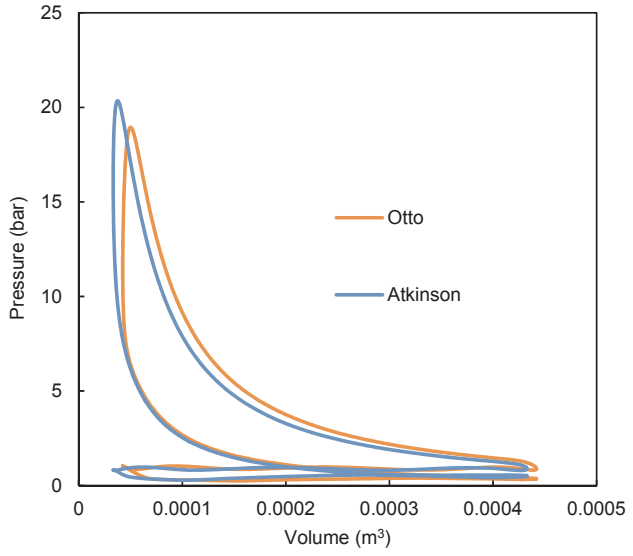

(a) 2000rpm@2bar

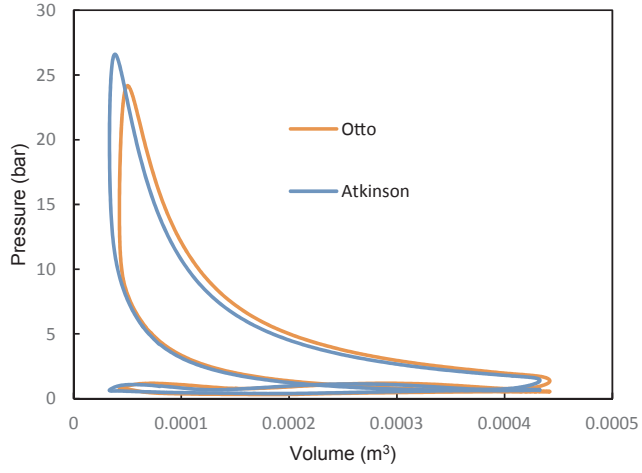

(b) 3000rpm@3bar

Fig. 15. Comparison of *P–V* diagram.

compared with the original engine, the crank angle of P_{max} decreases. The Atkinson cycle engine can achieve more obvious constant volume combustion and higher peak pressure, hence improves the thermal efficiency.

The comparison of CA50 and crank angle of P_{max} is shown in Fig. 16. The CA50s of Atkinson cycle engine locate in between 7 and 9 °CA ATDC and do not differ much compared with the original engine. The crank angle of P_{max} of Atkinson cycle engine appears 3 °CA earlier and the P_{max} of the Atkinson cycle engine is higher. Therefore, the combustion quality of the Atkinson cycle engine is improved compared with the original engine.

4. Conclusions

In this study, a novel optimization strategy of Atkinson cycle gasoline engine is proposed by combining thermodynamic analysis and one-dimensional simulation. The fuel-saving mechanism of Atkinson cycle engine is also deeply analyzed. These findings can be used as guidelines for the development of new Atkinson cycle engines. The main conclusions are as follows:

1) Atkinson cycle has the significant advantage of cycle efficiency at all pressure rise ratios, especially at high pressure rise ratio. The pressure rise ratio and the ratio of expansion ratio to effective compression ratio have significant influence on Atkinson cycle. At a fixed pressure rise ratio, the Atkinson efficiency first increases to a maximum value and then decreases with the increase of $\varepsilon_e/\varepsilon_c$.
2) The optimization strategy of Atkinson cycle engine is proposed. The range of compression ratio is preliminarily determined according to the Atkinson cycle efficiency at small pressure rise ratio through thermodynamic analysis; the optimization of the IVC at compression ratios is presented under the compression pressure constraint and the compression ratio and other valve timing are optimized through one-dimensional simulation.
3) Significant improvements in pumping losses and fuel economy are achieved, which verifies effectiveness of the present optimization strategy. The increase of mechanical efficiency due to the PMEP reduction is the main reason for the fuel economy improvement at low and medium load, while the increase of indicated thermal efficiency is the main reason for the fuel economy improvement at high load.
4) The BSFC of the Atkinson cycle engine is improved by 9% at 2000 rpm@2 bar and 8% at 3000 rpm@3 bar. The increase in intake pressure is the main reason for the decrease in PMEP. The Atkinson cycle engine can achieve more obvious constant volume combustion

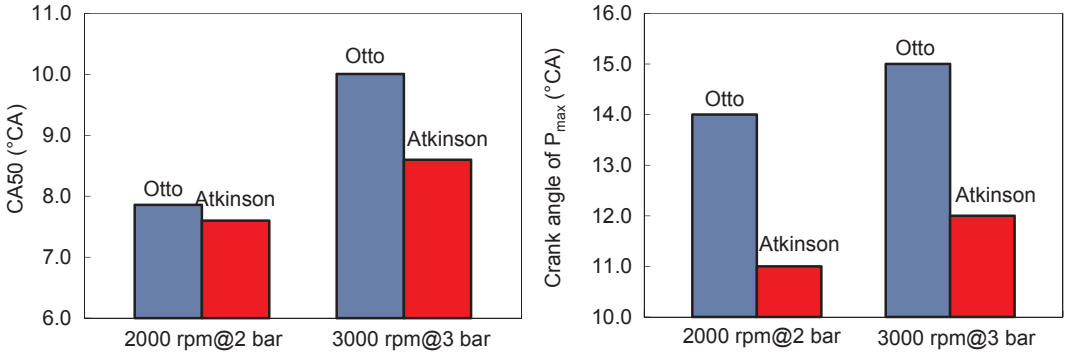

(a) CA50 (b) Crank angle of P_{max}

Fig. 16. Comparison of combustion characteristic parameters.

and the combustion quality has been greatly improved.

Atkinson cycle engine with high efficiency has become a popular choice for HEV and has a wide prospect. Further research will be carried out in the following aspects: the power performance, emission performance and the effectively use of intake reflux effect will be studied by exploring the working process of multi-cylinder Atkinson cycle engine.

CRediT authorship contribution statement

Qingyu Niu: Investigation, Software, Validation, Data curation, Formal analysis. Writing - original draft. **Baigang Sun:** Conceptualization, Methodology, Writing - review & editing. **Dongsheng Zhang:** Supervision. **Qinghe Luo:** Writing - review & editing.

Declaration of Competing Interest

The authors declare that they have no known competing financial interests or personal relationships that could have appeared to influence the work reported in this paper.

References

[1] Miklanek L, Vitek O, Gotfryd O, Klir V. Study of unconventional cycles (Atkinson and Miller) with mixture heating as a means for the fuel economy improvement of a throttled SI engine at part load. SAE technical paper no. 2012-01-1678. 2012.
[2] Muta K, Yamazaki M, Tokieda J. Development of new-generation hybrid system THS II – drastic improvement of power performance and fuel economy. SAE technical paper no. 2004-01-0064. 2004.
[3] Takahashi D, Nakata K, Yoshihara Y, Ohta Y, Nishiura H. Combustion development to achieve engine thermal efficiency of 40% for hybrid vehicles. SAE technical paper no. 2015-01-1254. 2015.
[4] Yonekawa A, Ueno M, Watanabe O, Ishikawa N. Development of new gasoline engine for ACCORD plug-in hybrid. SAE technical paper no. 2013-01-1738. 2013.
[5] Wang PY, Hou SS. Performance analysis and comparison of an Atkinson cycle coupled to variable temperature heat reservoirs under maximum power and maximum power density conditions. Energy Convers Manage 2005;46(15–16):2637–55.
[6] Hou SS. Comparison of performances of air standard Atkinson and Otto cycles with heat transfer considerations. Energy Convers Manage 2007;48:1683–90.
[7] Gonca G. Thermodynamic analysis and performance maps for the irreversible dual Atkinson cycle engine (DACE) with considerations of temperature-dependent specific heats, heat-transfer and friction losses. Energy Convers Manage 2016;111:205–16.
[8] Martins JJG, Uzuneanu K, Ribeiro BS, Jasasky O. Thermodynamic analysis of an over expanded engine. SAE technical paper no. 2004-01-0617. 2004.
[9] Mikalsen R, Wang YD, Roskilly AP. A comparison of Miller and Otto cycle natural gas engines for small scale CHP applications. Appl Energy 2009;86(6):922–7.
[10] Zhao YR, Chen JC. Performance analysis and parametric optimum criteria of an irreversible Atkinson heat-engine. Appl Energy 2006;83:789–800.
[11] Zhao J, Li Y, Xu F. The effects of the engine design and operation parameters on the performance of an Atkinson engine considering heat-transfer, friction, combustion efficiency and variable specific-heat. Energy Convers Manage 2017;151:11–22.
[12] Wei S, et al. Research on effects of early intake valve closure (EIVC) miller cycle on combustion and emissions of marine diesel engines at medium and low loads. Energy 2019;173:48–58.
[13] Zhao JX, Xu M, Li M, Wang B, Liu SZ. Design and optimization of an Atkinson cycle engine with the artificial neural network method. Appl Energy 2012;92:492–502.
[14] Li YT, et al. Realization of variable Otto-Atkinson cycle using variable timing hydraulic actuated valve train for performance and efficiency improvements in unthrottled gasoline engines. Appl Energy 2018;222:199–215.
[15] Li T, Gao Y, Wang JS, Chen ZQ. The Miller cycle effects on improvement of fuel economy in a highly boosted, high compression ratio, direct-injection gasoline engine: EIVC vs. LIVC. Energy Convers Manage 2014;79:59–65.
[16] Molina S, García A, et al. Miller cycle for improved efficiency, load range and emissions in a heavy duty engine running under reactivity controlled compression ignition combustion. Appl Therm Eng 2018;136:161–8.
[17] Wei HQ, Shao AF, et al. Effects of applying a Miller cycle with split injection on engine performance and knock resistance in a downsized gasoline engine. Fuel 2018;214:98–107.
[18] Mallikarjuna JM, Ganesan V. Theoretical and experimental investigations of extended expansion concept for SI engines. SAE technical paper no. 2002-01-1740. 2002.
[19] Cao YD. Thermodynamic cycles of internal combustion engines for increased thermal efficiency, constant-volume combustion, variable compression ratio, and cold start. SAE technical paper no. 2007-01-4115. 2007.
[20] Zaccardi JM, Pagot A, Vangraefschepe F, Dognin C, Mokhtari S. Optimal design for a highly downsized gasoline engine. SAE technical paper no. 2009-01-1794. 2009.
[21] Gheorghiu V. CO_2 emission reduction by means of enhancing the thermal conversion efficiency of ICE cycles. SAE technical paper no. 2010-01-1511. 2010.
[22] Watanabe S, Koga H, Kono S. Research on extended expansion general-purpose engine theoretical analysis of multiple linkage system and improvement of thermal efficiency. SAE technical paper no. 2006-32-0101. 2006.
[23] Westbrook CK, Mizobuchi Y, et al. Computational combustion. Proc Combust Inst 2005;30:125–57.
[24] Matsuo S, Ikeda E, Ito Y, Nishiura H. The new Toyota engine for hybrid car. SAE technical paper no. 2016-01-0684. 2016.
[25] Ohn H, Yu S, Min K. Spark timing and fuel injection strategy for combustion stability on HEV powertrain. Contr Eng Pract 2010;18:1272–84.
[26] Pertl P, Trattner A, Stelzl R, et al. Expansion to higher efficiency-experimental investigations of the Atkinson cycle in small combustion engines. SAE technical paper no. 2015-32-0809. 2015.
[27] Zhao JX, et al. Improving the partial-load fuel economy of 4-cylinder SI engines by combining variable valve timing and cylinder-deactivation through double intake manifolds. Appl Therm Eng 2018;141:245–56.
[28] Ricardo WAVE theory manual, version, 2009.
[29] Ricardo WAVE user guide, version, 2009.
[30] Anderson MK, Assanis DN, Filipi Z. First and second law analyses of naturally-aspirated, Miller cycle, SI engine with late intake valve close. SAE technical paper no. 980889. 1998.
[31] Blakey SC, Saunders RJ, Ma TH, Chopra A. A design and experimental study of an Otto Atkinson cycle engine using late intake valve closing. SAE technical paper no. 910451. 1991.